PJEST

First Principle Calculations of Structural, Electronic and Magnetic Properties of Mn Doped ZnS

Hafiz Tayyab Mahmood[1], Muhammad Amin[1], Azeem Nabi[2,3], Asghar Ali[1], Babur Zahir[1], Tahir Arshad[1], Anwar ul Haq[1,4]

[1]Department of Physics, University of Lahore, Lahore, Pakistan
[2]Department of Physics, University of Gujrat, Gujrat, Pakistan
[3]Department of Physics and Applied Mathematics, Pakistan Institute of Engineering and Applied Sciences, Nilore, Islamabad, Pakistan
[4]Department of Physics, University of Management and Technology, Lahore
Corresponding Authors: anwarskp@gmail.com, muhammad.amin@phys.uol.edu.pk

Abstract: In the present research work, a TBmBJ Exchange-Correlation Functional has been utilized to compute the spin polarized density functional theory. Various properties like structural, electronic as well as magnetic have been computed of $Zn_{1-x}Mn_xS$ (x= 50%, 25%, 12.5% and 6.25%). The present computed values of bandgap using TBmBJ matched well with the experimental results. Due to strong p-d hybridization, ferromagnetic exchange interactions between Mn -3d atom states are studied via S atom and magnetic moments are measured of these atoms. The exchange splitting parameters $N_0\alpha$ and $N_0\beta$ are analysed to verify the existence of ferromagnetism. Mn doped ZnS compositions display an n-semiconductor behavior. The presence of d-states at the upper edge of the valence band suggests that the studied materials are very good candidates to fabricate the magneto -optical devices.

Keywords: TB -mBJ; Exchange Splitting constant; Ex-change interactions; Ferromagnetism; Optical devices

Citation: Hafiz Tayyab Mahmood, Muhammad Amin, Azeem Nabi, Asghar Ali, Babar Zaheer, Tahir Arshad, & Anwar ul Haq. (2025). First Principle Calculations of Structural, Electronic and Magnetic Properties of Mn Doped ZnS. Pakistan Journal of Emerging Science and Technologies.

https://doi.org/10.5281/zenodo.17774431

Academic Editor: Dr. M. Javaid Afzal

Received date: 21-08-2025
Revised date: 26-11-2025
Accepted date: 27-11-2025
Published date: 03-12-2025

1. Introduction

Semiconductors have shown tremendous revolution in the field of science and technology and bring noteworthy development to enhance the worth of life and improvement in the industrial world. In scientific field, semiconductor has emerged rapidly growing technology to fabricate individual atom or molecule for devices. Now-a-days materials science has great revolution at an accelerating rate due to some application of materials in electronic, optoelectronics, spintronic, and some other devices. Scientists made great effort to explain diluted magnetic semiconductors (DMSs) at standard temperature to achieve ferromagnetism. In the semi-magnetic semiconductors (SMSCs) or spintronic, the DMSs plays a tremendous role [1]. In (DMSs) or (SMSs), the controlled amount of cation can take place magnetic ions [2]. Half-metallic ferromagnetic (HMFs) are most significant material in his family. To transfer and storage of information the magnetic moment and intrinsic spin of electron is used. The most effective usage of II–VI compound semiconductors are in solar cells, photovoltaic cells, light emitting diodes, memory storage devices, detectors, and spintronic devices. Many inorganic compounds are used for their optical, electro-physical, physiochemical and some other properties like light emitting diodes, biological sensors and solar cells etc. Non-magnetic nature of II-VI compound semiconductors is made ferromagnetic by replacing magnetic ions in II-VI semiconductors. Concentration of magnetic ions control the primary properties like

band gap, lattice constant, bond length and effective mass of II-VI semiconductors [3]. Zinc sulfide (ZnS) is a member of II-VI semiconductor. The calculated band gap of bulk cubic zincblende structure is 3.54 eV [4]. ZnS is one of the important materials with the extensive range of application such as laser devices, flat panel displays, photo-catalysis, ultraviolet light emitting diodes, optical devices, non-linear optical devices, cathode ray tube and antireflection coating [5].

In 3d transition metals, Mn contain half-filled 3d -shell which is most frequently use d material and have two 4 s 2 valance electrons. Mn atom transfer their two outermost electrons 4 s 2 to the anion host material and form ionic Mn+2. Mn with WZ structure or stable ZB is highly soluble in the host II -VI materials [6]. Mn with its half-filled 3d -shell and two valance electrons 4s 2 need extensive energy to add single electron, so 3d 5 orbit of Mn acts similar to 3d10 orbit chemically. The addition of Mn yields interesting results like optical and electrical properties as well as sp -band electrons and magnetic moment of the material. In 1980 the transition metals were largely studied by Blinowski [7]. Zinc sulfide (ZnS) is an important member of II -VI compounds semiconductor with a large band gap and outstanding photoelectric properties. It consists of two crystal structures, first cubic Zincblende structure owing bulk energy gap equal to 3.54 eV, secondly, the hexagonal crystal structure of energy gap of 3.91 eV [8]. Because of the large band gap energy ZnS is the most important host material for the electroluminescent devices [9]. ZnS exhibits potential applications in flat panel displays, solar energy conversion, catalysts, injection lasers, light emitting diodes and many others, due to its good transmittance and low dispersion in the infrared and visible range [10]. The electronic, structural, and magnetic properties of DMS of $Zn_{1-x}Mn_xS$ were studied by the R.Nouri et. al in their research paper they present the excessive potential application in magneto -electronic devices, spintronic materials technology and optoelectronic devices. They also present the physical properties of ZnS and $Zn_{1-x}Mn_xS$ based on the FP -LAPW by the first principles method within the advance WC: GGA potential. The magnetic optimization results indicate that the more stable state is displayed by the antiferromagnetic configuration [11]. Mahmood and Murtaza explored the structural, magnetic, mechanical, electronic and optical features of the phase of three $Zn_{1-x}V_xS$ alloys ferromagnetic semiconductor with different compositions with the ZB structure by using the first principle calculations. They studied all these properties in the frame work of DFT with the help of FPLAPW and local orbital. In their research paper they also indicate the deep knowledge to design and fabricate the optical and spintronic devices by using the investigated composition [12]. Huang et al. studied the optical characteristics, the electronic states along with the band structure of Cr-doped ZnS double-wall nanotubes through the first principle calculations within the frame of DFT using GGA+U potential. The computed optical and electronic results were found to be improved as a consequence of doping of Cr , which can have the potential applications in flat panel displays, photo-catalysis, ultraviolet light-emitting diodes and solar energy conversion. [13]. Mahmood et al. using the first principle calculation, examined the

optoelectronic, mechanical, magnetic, and structural properties of Cu doped ZnS and ZnSe compounds. In their research paper they elaborated that the ferromagnetic states have higher stability than the anti-ferromagnetic states. They showed that the absorption is maximum with minimum optical loss near the ultraviolet and in visible regions, which possibly makes these materials significant for the applications of electronic and optoelectronic devices [14]. The optoelectronic, structural and magnetic properties of V-doped Zincblende ZnS were explored using Perdew Burke Ernzerhz (PBE) exchange correlation functional through spin-polarized DFT by applying the GGA potential [15-17]. In this research work, keeping in view the studied literature mentioned above, zinc sulfide (ZnS) $Zn_{1-x}Mn_xS$ with different concentrations of Mn were selected to study their structural, electronic and magnetic characteristics using density functional theory[18-21]. The literature inspection aims that no reliable research paper was found for the present composition using TB - mBJ for its band gap engineering. The consequences analysed during this research work are very fascinating and noteworthy for discovering the behavior of Mn:ZnS material and its function in the optoelectronic devices. The results obtained in this study are both compelling and important for understanding the material's potential in spintronics, magneto-optical, and optoelectronic device applications.

2. Computational details

Within the TB-mBJ approach, DFT-based first-principles computations were used to determine the electronic structure and magnetic response of Mn-substituted ZnS. A cubic structure with space group number 216 (F43m) of 8 -atom, 16 -atom, 32 -atom and 64 -atom with doping concentration of 50%, 25%, 12.5% and 6.25% in each supercell. The Brillouin zone k -point sampling was performed using 3 × 3 × 3 k -mesh. We carefully chosen the muffin –tin radii (MT) for Zn, S and Mn to be 2.2, 1.9 and 1.9 a.u., correspondingly. The electron configurations of Zn are [Ne]3s 2 3p 6 3d104s 2, S is [Ne] 3s 2 3p 4, and Mn is [Ne]3s 2 3p 6 3d 5 4s 2 . To determines matrix size (convergence), the parameter RMT×Kmax=8, where Kmax is the plane wave cut -off and the smallest of all atomic sphere radii is RMT [22]. To optimize the internal atomic positions, the energy, gradient, and convergence criteria were set to 10^{-5} eV, 10^{-4} eV/Å, and 10^{-3} eV, respectively. All atomic positions were fully relaxed in these calculations.

3. Results and discussion

In this article, the first principle calculations were carried out by using WIEN2k code [22] to find the electronic, structural and magnetic characteristics of Mn: ZnS with different impurity concentrations. The calculated results are discussed in detail and are given below;

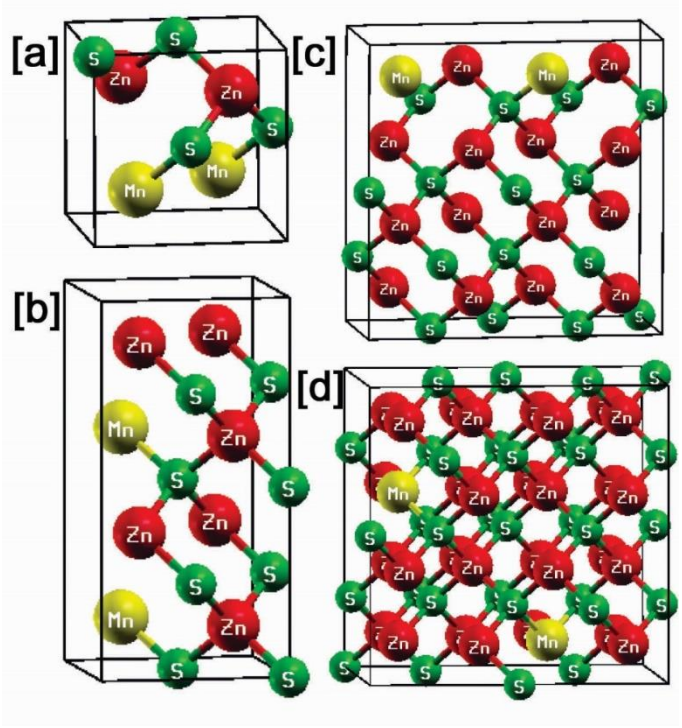

Fig 1: Supercell of (a) 8-atoms (b) 16-atoms (c) 32-atoms and (d) 64-atoms

Fig. 1 Shows the super cell of (a) 8-atoms (b)16-atoms (c) 32-atoms and (d) 64-atoms with doping concentration of 2-atom in each supercell. The bond lengths are also calculated and the values of bond lengths between 8-atoms, 16-atoms,32-atoms and 64-atoms are listed in Table 1.

The bond lengths between 8 -atom, 16 -atom, 32 -atom and 64 -atom, between Zn -S are 2.33, 2.35, 2.34, and 2.35, between Zn -Mn are 3.83 eV, 3.83 eV, 3.85 eV and 3.84 eV, and between Mn -S are 2.37, 2.36, 2.37 and 2.38 respectively. The value of electronegativity for Zn, S and Mn are 1.65, 2.58 and 1.55 respectively. The electronegativity difference between Mn -S, Zn - S and Mn -Zn is 1.03, 0.93 and 0.1 (Pauling scale) respectively. The values between 0.5 to 1.7 (Pauling scale) are referred as polar bond so the bond between Mn -S and Zn -S are referred as partially ionic and partially covalent bonds. However, the bond between Mn -Zn is covalent in nature.

Table .1: Bond lengths Mn:ZnS

Bond length	8-atom	16-atom	32-atom	64-atom
Zn-S	2.33	2.35	2.34	2.35
Zn-Mn	3.83	3.83	3.85	3.84
Mn-S	2.37	2.36	2.37	2.38

3.1 Electronic Properties

3.1.1 Density of states

To determine the carrier density in a semiconductor, we first need to identify the number of available states at each energy level. Next, the No. of states and the probability that an electron would occupy a state are multiplied to get the number of electrons. The number of states per unit of energy and per unit volume will be computed since the size of the semiconductor affects the amount of energy levels [16]. Table 2 displays density of states for supercell of 8 -atom, 16 -atom, 32 -atom and 64 -atom. The estimated band gap values are 3.4 eV, 3.7 eV, 3.67 eV and 3.66 eV in spin up channel and 3.83eV, 3.91eV, 3.88 eV and 3.91 eV in spin down channel is consistent with experimental value of band gap 3.70 eV [25], respectively.

Table 2: Band gap values of Mn: ZnS

Band gap	8-atom	16-atom	32-atom	64-atom
Spin-up	3.4	3.7	3.67	3.66
Spin-down	3.83	3.91	3.88	3.91

Fig. 2 demonstrates the total density of states (DOSs) for 8-atom, 16-atom, 32-atom and 64-atom super cells. The DOSs clearly shows that in spin-up channel, the band gap is 3.4 eV, 3.7 eV, 3.67 eV and 3.66 eV and 3.83 eV, 3.91 eV, 3.88 and 3.91 eV in spin down channel, respectively. The fermi-level is set to zero. In the valence band there is hybridization between anion Sulphur (S) s-states and Zn-4s, Zn-3p and Zn-3d, these are bonding states and are responsible for the formation of valence band as shown in Fig. 3. The conduction bands have Zn - 4s and a mixture of Mn -3d and Zn - 4s states for spin down channel [23-25].

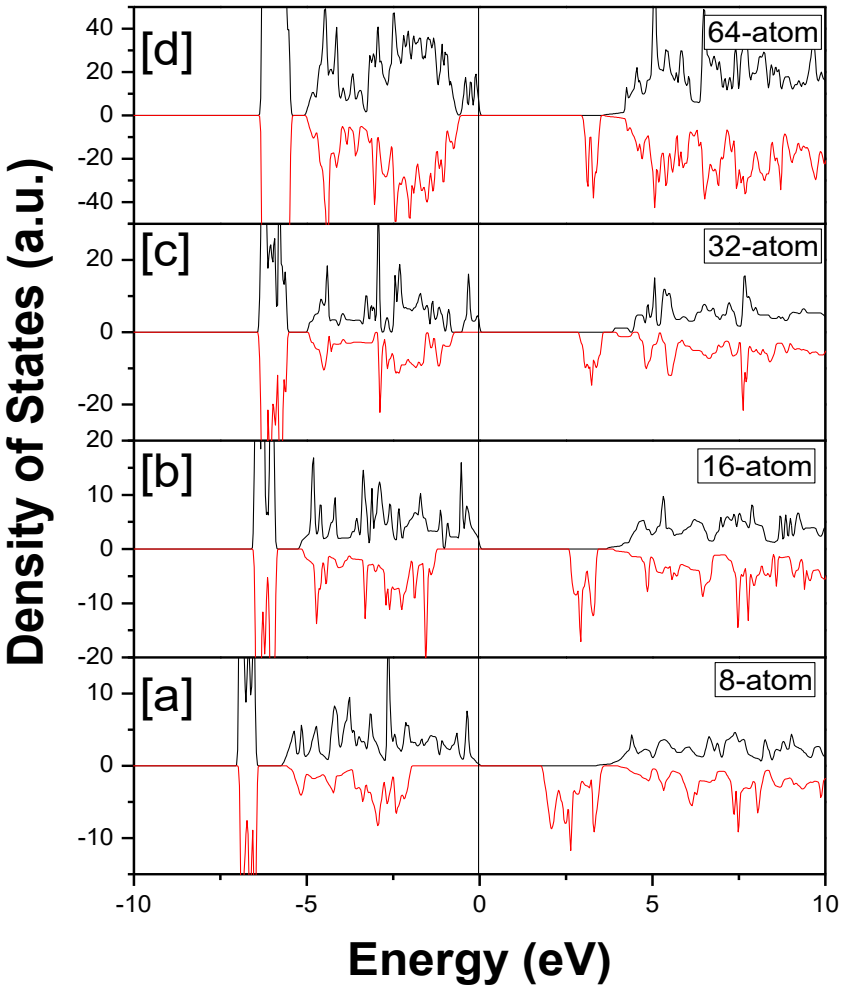

Fig 2: Total Density of states of (a) 8-atom (b) 16-atom(c) 32-atom and (d) 64-atom super cell

In Mn 3d states, the spin-down channel is populated, while the spin-up channel remains empty. The DOSs in spin -up channel show that some states are present at the top of spin up valence band, hence the material is p-type semiconductor. As the size of supercell increases the width of band available at top of valence band keep on decreasing with the decrease in impurity concentration. So, this is a confirmation that only d-states are available at the top of valence band. This needs to discuss these states (Mn-3d) in more detail.

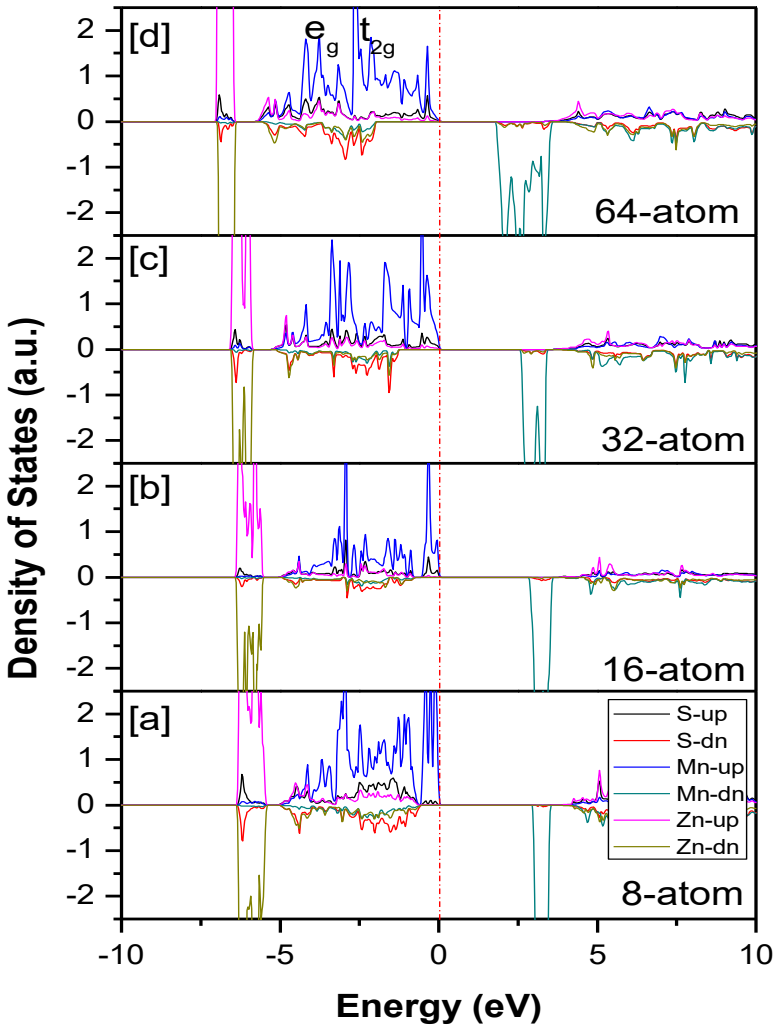

Fig 3: Partial density of states for ZnS and Mn for (a) 8 -atom (b)16 -atom(c) 32 -atom and (d) 64 -atom super cells

The cubic structure can split into eg and t2g states under the effect of tetrahedral crystal field, the t2g states can strongly hybridize to form p -d orbitals. Fig. 3 shows that Mn -3d states are split into doubly degenerate (e g) and triply degenerate states (t2g) under the effect of crystal field splitting, which are further split under the effect of John Teller Distortion [26 -28]. The partial DOSs shows that for 8 -atom, 16 -atom, 32 -atom and 64 -atom supercell, the Mn states are present at the top of valence band in spin -up channel. The pd -hybridization is present between Mn -3d states and S -p states. Some Mn -3d states that are present at bottom of conduction band in spin down channel. It is also clear from band structure diagram as shown in Fig. 4 that doubly degenerate states (non -bonding) are present at the top of valence band.

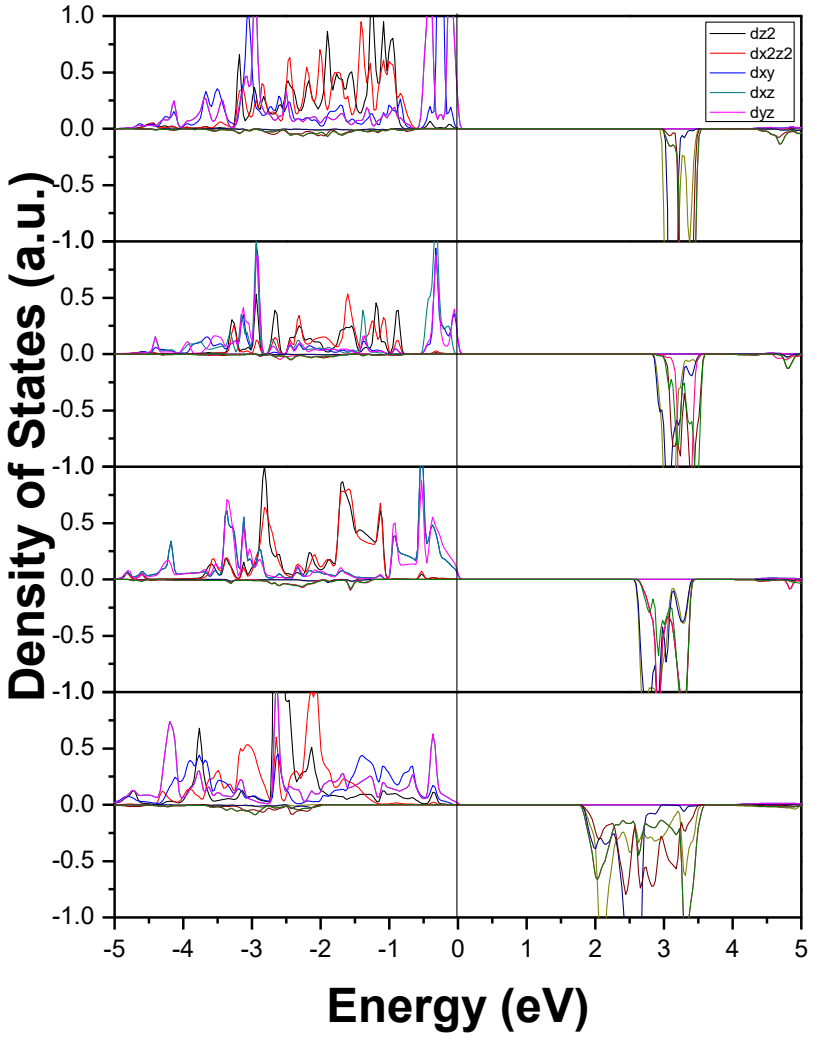

Fig 4: Mn –d Partial density of states for (a) 8-atom (b) 16-atom(c) 32-atom and (d) 64-atom supercells

3.1.2 Band Structure

From band structure diagram displayed in Fig. 5, it is obvious that Mn -doped ZnS at different impurity concentrations are direct band gap semiconductors with band gap of 3.4 eV, 3.7 eV, 3.67 eV and 3.66 eV in spin up [25] channel and 3.83eV, 3.91eV, 3.88 and 3.91eV in spin down channel, respectively. The values of splitting of valence band maxima and conduction band minima are given in table 2. In spin up channel the Mn -3d states are present at the top of valence band, these states are responsible to tune the optical properties of material by changing the value of impurity concentration. Due to these states at top of valence band the value of band gap is also decreased.

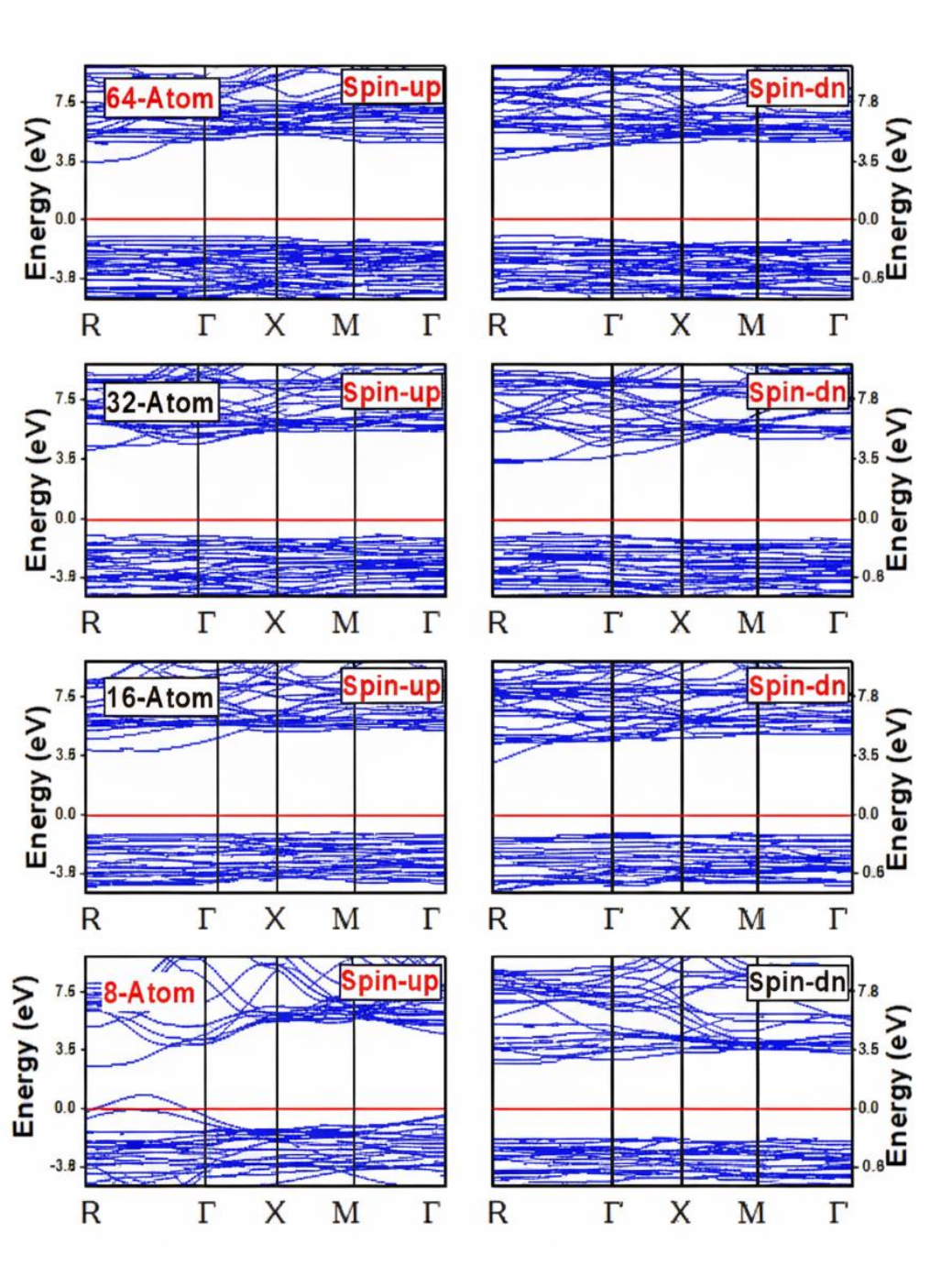

Fig 5: Band structures plots for (a) 8-atom (b)16-atom(c) 32-atom and (d) 64-atom supercells

3.2 Magnetic Properties

We have also calculated the spin-exchange splitting energy, Δxd, derived from the band structure diagram. This energy is characterized by the distance between the respective spin-up and spin-down peaks. Additionally, our discussion includes an analysis of the p-d exchange splitting, denoted as: $\Delta(pd) = Ev\downarrow - Ev\uparrow$ and $\Delta xc(pd) =$

$Ec\downarrow - Ec\uparrow$, as well as the exchange parameters $N_0\alpha$ and $N_0\beta$ [23], which are described as follows

$$\boldsymbol{N_o\,\alpha} = \Delta\, Ec\,/x\,\langle\, s\,\rangle \qquad (1)$$

$$\boldsymbol{N_o\,\beta} = \Delta\, Ev\,/x\,\langle\, s\,\rangle \qquad (2)$$

Here, ΔEc and ΔEv represent the band edge splitting of the conduction band and valence band, respectively, while $x\langle s\rangle$ denotes half the magnetization per TM atom. All these calculated values are provided in Table 4.

Table 3: Magnetic moments on Mn, Zn and S atoms

Mn:ZnS	**8-atom**	**16-atom**	**32-atom**	**64-atom**
Zn	0.41	0.02	0.009	0.0040
S	0.65	0.03	0.028	0.0035
Mn	4.39	4.33	4.34	4.3700

Table 4: Exchange splitting constants Mn:ZnS

Mn:ZnS	**8-atom**	**16-atom**	**32-atom**	**64-atom**
$\Delta^{c}{}_{x}$(pd)	-1.111	-0.597	-0.431	-0.273
$\Delta^{v}{}_{x}$(pd)	1.986	1.028	0.667	0.514
$N_{o\alpha}$	-11.11	-2.985	-1.077	-0.341
$N_{o\beta}$	19.86	5.150	1.663	0.643

The effective potential for the majority spin in this system is significantly more favorable and attractive than that of the minority spin, as indicated by the negative value of $\Delta\,(pd)$ for Mn:ZnS. A decrease in impurity concentration and an increase in supercell size are correlated with an increase in Noα value. The value of Noβ decrease with decrease in impurity concentration and increase in supercell size. We have computed these exchange parameters at a lower Mn concentration of 6.25%, whereas prior research was conducted at a much higher concentration level of 25% in ZnS [24, 29,30].

Conclusion

In this research work a model potential TB-mBJ is used to analyze the electronic, magnetic and structural characteristics of ZB Mn:ZnS at different doping concentration of 50%, 25%, 12.5% and 6.25%. Mn:ZnS photoluminescence is caused by the introduction of particular non-bonding and anti-bonding states near the top of the valence band by Mn doping. The magnetic moment value was determined to be 4.37 μB and the magnetism primarily originating from the Mn-3d impurity atom. Permanent magnets were formed as a result of p-d hybridization, which was shown to lower the Mn local magnetic moment relative to its free space charge value and to induce tiny local magnetic moments on the non-magnetic Zn and S host sites, which are aligned parallel to the Mn atom. Moreover, the presence of d-states at top of valence band give rise to photo-luminescence properties and the constants N0α, N0β and exchange splitting verify that ferromagnetism exits in Mn:ZnS, therefore the material is suitable for magneto-optical devices and our findings are consistent with experimental available literature.

Author's Contribution: H.T.M. & M.A., Conceived the idea; A.N. & A.A. Designed the simulated work or acquisition of data; B. Z., Executed simulated work, data analysis or analysis and interpretation of data and wrote the basic draft; T.A & A.U.H, Did the language and grammatical edits or Critical revision

Funding: The publication of this article was funded by no one.

Conflicts of Interest: The authors declare no conflict of interest.

Acknowledgment: The authors would like to thank the advisors who advised for assistance with the collection of data.

References

[1] A. Brandlmaier, S. Geprägs, G. Woltersdorf, R. Gross, and S. Goennenwein, "Nonvolatile, reversible electric-field controlled switching of remanent magnetization in multifunctional ferromagnetic/ferroelectric hybrids," *J. Appl. Phys.*, vol. 110, no. 4, p. 043913, 2011. https://doi.org/10.1063/1.3624663

[2] S. Aksu, E. Bacaksiz, M. Parlak, S. Yılmaz, I. Polat, M. Altunbaş, M. Türksoy, R. Topkaya, and K. Özdoğan, "Structural, optical and magnetic properties of Mn diffusion-doped CdS thin films prepared by vacuum evaporation," *Mater. Chem. Phys.*, vol. 130, no. 1–2, pp. 340–345, 2011. https://doi.org/10.1016/j.matchemphys.2011.06.046

[3] S. Pearton, C. Abernathy, M. Overberg, G. Thaler, D. Norton, N. Theodoropoulou, A. Hebard, Y. Park, F. Ren, and J. Kim, "Wide band gap ferromagnetic semiconductors and oxides," *J. Appl. Phys.*, vol. 93, no. 1, pp. 1–13, 2003. https://doi.org/10.1063/1.1517164

[4] K. Liu, J. Li, Y. Xu, H. Li, and W. Gao, "Investigation of ZnS films prepared with different solvents and zinc sources under different experimental conditions," *Results Phys.*, vol. 11, pp. 749–754, 2018. https://doi.org/10.1016/j.rinp.2018.10.015

[5] L. B. Chandrasekar, R. Chandramohan, R. Vijayalakshmi, and S. Chandrasekaran, "Preparation and characterization of Mn-doped ZnS nanoparticles," *Int. Nano Lett.*, vol. 5, no. 2, pp. 71–75, 2015. https://doi.org/10.1007/s40089-015-0139-6

[6] D. A. Debrah, *Molecular Modeling of Dirhodium Complexes*. Johnson City, TN, USA: East Tennessee State Univ., 2014. Available: https://dc.etsu.edu/etd/2426/

[7] J. Blinowski, P. Kacman, and J. Majewski, "Ferromagnetism in Cr-based diluted magnetic semiconductors," *J. Cryst. Growth*, vol. 159, no. 1–4, pp. 972–975, 1996. https://doi.org/10.1016/0022-0248(95)00719-9

[8] K. Liu, J. Li, Y. Xu, H. Li, and W. Gao, "Investigation of ZnS films prepared with different solvents and zinc sources under different experimental conditions," *Results Phys.*, vol. 11, pp. 749–754, 2018. https://doi.org/10.1016/j.rinp.2018.10.015

[9] D. Patidar, R. Sharma, N. Jain, T. Sharma, and N. Saxena, "Optical properties of CdS sintered film," *Bull. Mater. Sci.*, vol. 29, no. 1, pp. 21–24, 2006. https://doi.org/10.1007/BF02709350

[10] R. Sahraei and S. Darafarin, "Preparation of nanocrystalline Ni doped ZnS thin films by ammonia-free chemical bath deposition method and optical properties," *J. Lumin.*, vol. 149, pp. 170–175, 2014. https://doi.org/10.1016/j.jlumin.2014.01.040

[11] R. Nouri, R. Belkacemi, M. Ziane, S. Ghemid, R. Chemam, and H. Meradji, "The reciprocal correlation between magnetic and structural, electronic, optical properties of DMS of Zn1–xSMnx," *Optik*, vol. 168, pp. 901–912, 2018. https://doi.org/10.1016/j.ijleo.2018.05.021

[12] Q. Mahmood, G. Murtaza, R. Ahmad, T. Hussain, and I. Will, "First principle study of vanadium doped ZnS: Structural, electronic, elastic, magnetic and optical properties using mBJ approximation," *Curr. Appl. Phys.*, vol. 16, no. 3, pp. 361–370, 2016. https://doi.org/10.1016/j.cap.2015.12.024

[13] Y. Huang, Z. Zhang, F. Ma, P. K. Chu, C. Dong, and X. Wei, "First-principles calculation of the band structure, electronic states, and optical properties of Cr-doped ZnS double-wall nanotubes," *Comput. Mater. Sci.*, vol. 101, pp. 1–7, 2015. https://doi.org/10.1016/j.commatsci.2015.01.011

[14] Q. Mahmood, S. Alay-e-Abbas, M. Hassan, and N. Noor, "First-principles evaluation of Co-doped ZnS and ZnSe ferromagnetic semiconductors," *J. Alloys Compd.*, vol. 688, pp. 899–907, 2016. https://doi.org/10.1016/j.jallcom.2016.07.302

[15] M. El Amine Monir, H. Baltache, R. Khenata, G. Murtaza, R. Ahmed, W. K. Ahmed, and A. Bouhemadou, "Half-metallicity and optoelectronic properties of V-doped

zincblende ZnS and CdS alloys," *Int. J. Mod. Phys. B*, vol. 30, no. 8, p. 1650034, 2016. https://doi.org/10.1016/j.jallcom.2016.07.302

[16] M. Amin, A. ul Haq, G. M. Mustifa, A. Afaq, S. M. Ramay, R. Sharma, and A. Hanif, "Cs2TlRhX6 (X = Cl, Br, I): promising halide double perovskites for efficient energy harvesting in photovoltaic and thermoelectric applications," *Phys. Scr.*, vol. 98, no. 12, p. 125983, 2023. https://doi.org/10.1088/1402-4896/ad0e9a

[17] Ramay, S. M., ul Haq, A., Amin, M., Aslam, U., Mushtaq, T., Hanif, A., ... & Siddig, A. A. (2024). Computational study of narrow bandgap double halide perovskites Rb2TlRhX6 (X= Cl, Br, I) for energy harvesting applications. *Physica Scripta*, *99*(12), 125965. https://doi.org/10.1088/1402-4896/ad9098

[18] A. Es-Smairi, N. Fazouan, and E. H. Atmani, "A DFT insight into magnetic, optoelectronic and thermoelectric properties of h-Zn1-xCuxS monolayer," *Comput. Theor. Chem.*, vol. 1228, p. 114286, 2023. https://doi.org/10.1016/j.comptc.2023.114286

[19] A. A. Othman, M. A. Osman, M. A. Ali, and E. M. M. Ibrahim, "Influence of transition metals dopant type on the structural, optical, magnetic, and dielectric properties of ZnS nanoparticles prepared by ultrasonication process," *Mater. Sci. Eng. B*, vol. 270, p. 115195, 2021. https://doi.org/10.1016/j.mseb.2021.115195

[20] R. Nouri, R. Belkacemi, M. I. Ziane, S. Ghemid, R. Chemam, and H. Meradji, "The reciprocal correlation between magnetic and structural, electronic, optical properties of DMS of Zn1-xSMnx," *Optik*, vol. 168, pp. 901–912, 2018. https://doi.org/10.1016/j.ijleo.2018.05.021

[21] A. A. M'hid, G. Li, M. Boughrara, M. Kerouad, and Q. Wang, "Tuning the magnetic properties of doped ZnS using transition metal doping: A multi-scale computational approach," *Mater. Today Commun.*, vol. 38, p. 107825, 2024. https://doi.org/10.1016/j.mtcomm.2023.107825

[22] K. Schwarz, P. Blaha, and G. K. Madsen, "Electronic structure calculations of solids using the WIEN2k package for material sciences," *Comput. Phys. Commun.*, vol. 147, no. 1–2, pp. 71–76, 2002. https://doi.org/10.1016/S0010-4655(02)00206-0

[23] J. Kaczkowski and A. Jezierski, "DFT+U Calculations of Transition Metal Doped AlN," *Acta Phys. Pol. A*, vol. 116, no. 5, p. 924, 2009. https://doi.org/10.12693/aphyspola.116.924

[24] S. Nazir, N. Ikram, S. Siddiqi, Y. Saeed, A. Shaukat, and A. H. Reshak, "First principles density functional calculations of half-metallic ferromagnetism in Zn1-xCrxS and Cd1-xCrxS," *Curr. Opin. Solid State Mater. Sci.*, vol. 14, no. 1, pp. 1–6, 2010. https://doi.org/10.1016/j.cossms.2009.08.001

[25] S. F. Rabbani and I. S. Banu, "Half metallic ferromagnetism in (Mn, Cr) codoped ZnS dilute magnetic semiconductor: First principles calculations," *Comput. Mater. Sci.*, vol. 101, pp. 281–287, 2015. https://doi.org/10.1016/j.commatsci.2015.01.043

[26] G. Murugadoss, "Luminescence properties of co-doped ZnS: Ni, Mn and ZnS: Cu, Cd nanoparticles," *J. Lumin.*, vol. 132, no. 8, pp. 2043–2048, 2012. https://doi.org/10.1016/j.jlumin.2012.02.011

[27] B. Van Zeghbroeck, *Principles of Semiconductor Devices*. Boulder, CO, USA: Univ. Colorado, 2004. Available: https://truenano.com/PSD20/contents/table%20of%20contents.pdf

[28] S. Nazir, "First principles density functional calculations of half-metallic ferromagnetism in Zn1-xCrxS and Cd1-xCrxS," *Curr. Opin. Solid State Mater. Sci.*, vol. 14, no. 1, pp. 1–6, 2010. https://doi.org/10.1016/j.cossms.2009.08.001

[29] M. Yaseen, H. Ambreen, A. Sufyan, M. K. Butt, S. U. Rehman, J. Iqbal, M. Shamsa Bibi, A. Murtaza, and S. M. Ramay, "Optical and magnetic properties of manganese doped zinc sulphide: density functional theory approach," *Ferroelectrics*, vol. 557, no. 1, pp. 112–121, 2020. https://doi.org/10.1080/00150193.2020.1713356

[30] H. Van Bui, D. Van Thai, T. Dai Nguyen, H. T. Tran, N. D. Nui, and N. M. Hung, "Mn-doped ZnS nanoparticle photoanodes: Synthesis, structural, optical, and photoelectrochemical characteristics," *Mater. Chem. Phys.*, vol. 307, p. 128081, 2023. https://doi.org/10.1016/j.matchemphys.2023.128081